The influence of strained ZnTe islands on excitonic recombination and the self-organizing effects of ZnTe islands in a wide CdTe-based quantum well

1998 J. Phys.: Condens. Matter 10 1839

(http://iopscience.iop.org/0953-8984/10/8/016)

J. Phys.: Condens. Matter **10** (1998) 1839–1854. Printed in the UK PII: S0953-8984(98)89134-0

The influence of strained ZnTe islands on excitonic recombination and the self-organizing effects of ZnTe islands in a wide CdTe-based quantum well

Q X Zhao†‡, N Magnea‡ and M Willander†

† Physical Electronics and Photonics, Department of Physics, Chalmers University of Technology and Göteborg University, S-412 96 Göteborg, Sweden

‡ CEA/DRFMC/SP2M/PSC, 17 rue des Martyrs, 38054 Grenoble Cédex 9, France

Received 11 November 1997

Abstract. Structures consisting of ZnTe fractional monolayers embedded coherently in a CdTe quantum well are investigated by means of optical measurements. This study is designed to study the influence of the strained ZnTe islands on excitonic recombination and to explore the dependence of the self-organizing effects of the ZnTe island on growth temperatures. The experimental results show that the strained ZnTe islands can strongly modify the excitonic transitions related to the quantization of the excitonic centre-of-mass motion (CM quantization). We have shown that the striking increase of the effective g-factor of the CM quantized excitons is due to the change of the hole g-factor involved since it is found experimentally that the electron g-factor is unchanged. The experimental results also show that a coherent distribution of the ZnTe islands is formed at higher growth temperatures ($\geqslant$280 °C), while a random distribution of the ZnTe islands is formed at lower growth temperatures (=240 °C). A coherent alignment of the islands along the growth direction is concluded.

1. Introduction

The study of self-assembled quantum islands has attracted significant attention in recent years due to the interest in understanding the fundamental physics and the potential of realizing quantum dot laser structures directly. Experimental observations of the coherent growth of islands have been reported for InGaAs/GaAs [1–6] and SiGe/Si systems [7–9]. Theoretical simulations have shown a possible explanation as to why the self-assembled effects exist in a strained heterostructure [9, 10]. So far, most of the investigations have dealt with a system in which the islands show an attractive potential for electrons. Recent achievements in growing high-quality structures containing a fractional monolayer (ML) of highly strained ZnTe layers in a CdTe matrix [11–13] open up the possibility of studying an anti-dots system where the islands show a repulsive potential for electrons. According to the theoretical model applied to self-assembled islands in a strained system [5, 9, 10], the ordering effect in an anti-dots system (such as CdTe/ZnTe) is also expected as long as there is an inhomogeneous surface potential. If such an ordering effect exists, then it should be reflected in the change in the optical properties in a quantum well in which several fractional monolayers of highly strained material are embedded, since excitons are very sensitive to the nature of potential fluctuations.

In this investigation, we will present a systematic study of structures containing fractional ML of ZnTe insertions in a CdTe matrix by both stationary and time-resolved

0953-8984/98/081839+16$19.50

optical measurements under a magnetic field or an electric field which act as perturbations. We will explore the correlation between the radiative excitonic recombination and the strained ZnTe islands, and we will study the correlation between the coherent ZnTe island formation and growth temperatures. To characterize the ZnTe (6.2% lattice mismatch with CdTe) islands by optical spectroscopy, we have chosen to monitor the excitonic transitions related to the quantization of the excitonic centre-of-mass motion (CM quantization) in a wide (∼78 nm) CdTe quantum well, because such mobile excitons are very sensitive to the coherent motion along the growth direction as well as to any disorder.

The paper is organized in the following way. In section 2, we first give a brief description of the sample structures and the experimental set-up. In section 3 we will discuss the properties of the excitons related to quantization of the excitonic centre-of-mass motion and present the experimental results obtained from optical measurements in the presence of applied magnetic and electric fields. Section 4 will focus on the influence of the strained ZnTe islands on excitonic recombination and the effects of growth temperatures. It can be seen that our optical data suggest the existence of a correlated distribution of the ZnTe islands along the growth direction at certain growth temperatures. Simple theoretical treatments are discussed in section 5, and finally a summary is given in section 6.

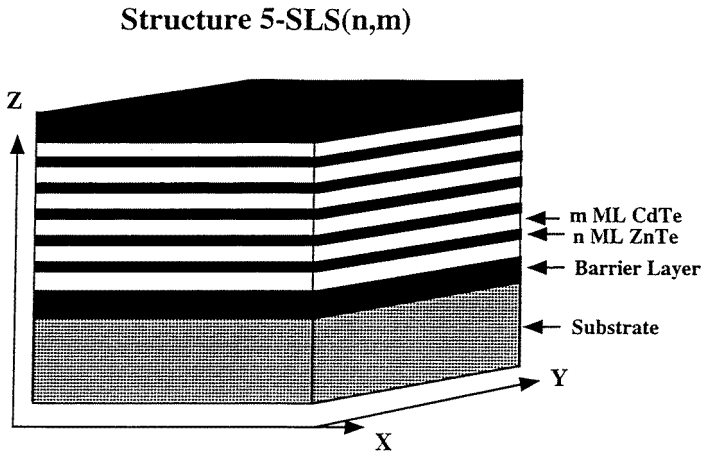

Figure 1. A schematic view of the structure corresponding to 5-SLS(n, m).

2. Samples and experimental details

Wide CdTe single-QW structures with multiple ZnTe insertions are grown on normal (001) $Cd_{0.96}Zn_{0.04}Te$ or $Cd_{0.95}Zn_{0.05}Te$ substrates by molecular beam epitaxy. The ZnTe layers are inserted evenly in CdTe well region. We denote such a short superlattice structure as j-SLS(m, n), where j is the number of ZnTe insertions, and m and n are the numbers of monolayers in the ZnTe insertion and in the CdTe layer separating two neighbouring ZnTe insertions, respectively. A schematic view of the structure 5-SLS(m, n) is shown in figure 1. The details of the samples used in this study are summarized in table 1. The thicknesses of the ZnTe and CdTe layers in these samples (which are indicated in table 1) are deduced from x-ray diffraction measurements.

Photoluminescence (PL), PL excitation (PLE), polarized PLE (PPLE) and transmission

Table 1. The structures (j-SLS(m, n)) used in this study. 1 ML_{ZnTe} = 0.305 185 nm; 1 ML_{CdTe} = 0.324 05 nm.

Sample	j	ZnTe m (ML)	CdTe n (ML)	Barrier material	Growth temperature T_s (°C)	Substrate material
Z882	5	0	40	$Cd_{0.75}Mg_{0.25}Te$	320	$Cd_{0.96}Zn_{0.04}Te$
Z881	5	0.6	43	$Cd_{0.75}Mg_{0.25}Te$	240	$Cd_{0.96}Zn_{0.04}Te$
Z879	5	0.8	40	$Cd_{0.75}Mg_{0.25}Te$	280	$Cd_{0.96}Zn_{0.04}Te$
Z887	5	0.8	42	$Cd_{0.75}Mg_{0.25}Te$	320	$Cd_{0.96}Zn_{0.04}Te$
Z855	5	0.35	37	$Cd_{0.92}Zn_{0.08}Te$	320	$Cd_{0.96}Zn_{0.04}Te$
Z927	5	0.6	40	$Cd_{0.92}Zn_{0.08}Te$	210	$Cd_{0.95}Zn_{0.05}Te$
Z852	3	0.48	49	$Cd_{0.92}Zn_{0.08}Te$	320	CdTe

measurements were carried out in an 8 T magnet in a Faraday configuration at 1.8 K. For the PL, PLE and PPLE measurements, a CW Ar^+-laser-pumped Ti:sapphire laser was used, and white light from a 100 W halogen projector lamp was used for the transmission measurements. In the PPLE measurements we used a photoelastic modulator, whereby the intensity difference between σ^+- and σ^--polarization can be measured. For the spin-quantum-beat measurements, the sample is mounted in a He gas flow cryostat in a superconducting magnet in the Voigt configuration with a magnetic field perpendicular to the growth direction of the QWs. The sample is excited in the growth direction by circularly polarized picosecond pulses from a mode-locked Ti:sapphire laser with a repetition rate of 80 MHz. The circularly polarized PL is detected in the backward direction by a streak camera. The time resolution is better than 10 ps.

3. The quantization of the excitonic centre-of-mass motion in a wide QW

The confinements of electrons and holes strongly depend on the well width and the band offset between the well and barrier layers. It is believed that the valence band offset (VBO) is about 30% [14] of the total band-gap difference between the CdTe and CdMgTe materials, and the difference of the band-gap energy between $Cd_{1-x}Mg_xTe$ alloy and CdTe is given by $\Delta E(x) = 1.75x$ (eV). For the $CdTe/Cd_{1-x}Zn_xTe$ system, the average valence band offset (the chemical valence band offset without strain plus the contribution of the hydrostatic stress energy) between CdTe and $Cd_{1-x}Zn_xTe$ is very small [15], and can be approximately taken as zero [15, 16]. The energy difference in band gap between $Cd_{1-x}Zn_xTe$ and CdTe is given by $\Delta E(x) = 0.525x + 0.26x^2$ (eV).

Figure 2 shows a schematic potential for electrons and holes in the CdTe/CdMgTe system. The wave functions for the first confined electron and hole states are also included in the figure. The heavy-hole (hh) and light-hole (lh) band-edge splitting in the CdTe well region is due to the strain effects introduced by a $Cd_{0.96}Zn_{0.04}Te$ substrate used in the structure. For the structures with CdZnTe as barrier layers, the potential profile for electrons and the heavy holes is similar to the CdTe/CdMgTe case (figure 2). The electron and the heavy-hole band offsets between the barrier layer and the CdTe well layer are 32 meV and 13 meV for the $CdTe/Cd_{0.92}Zn_{0.08}Te$ system (300 meV and 136 meV for the $CdTe/Cd_{0.75}Mg_{0.25}Te$ system), respectively. The light-hole potential is type II (−13 meV) between the $Cd_{0.92}Zn_{0.08}Te$ barrier layer and the CdTe well layer (this means that the light holes will be confined in $Cd_{0.92}Zn_{0.08}Te$ barrier layers), while it is type I (123 meV) between the $Cd_{0.75}Mg_{0.25}Te$ barrier layer and the CdTe well layer (as show in figure 2). For this

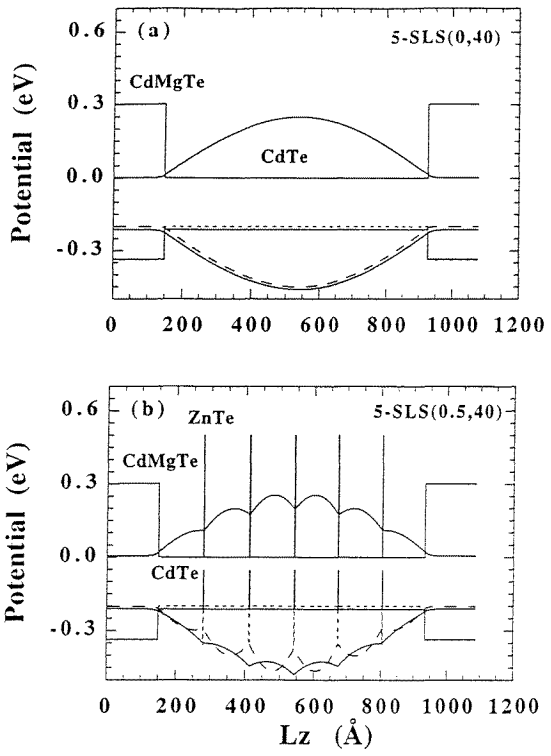

Figure 2. The potential for electrons (solid lines) and holes (solid lines for light holes and dotted lines for heavy holes) in the structures (a) 5-SLS(0, 40) and (b) 5-SLS(0.5, 40) grown on a $Cd_{0.96}Zn_{0.04}Te$ substrate, respectively. The wave functions of the first confined electron (solid lines) and hole states (solid lines for light holes and dashed lines for heavy holes) are also indicated in the figure, and the relative shift between the first heavy- and light-hole wave function in the CdMgTe barrier region represents the energy separation between these two bands. The separation between the CdTe conduction band (CB) and valence bands (VB) is fixed at 200 meV for reasons of clarity; otherwise the energy scale represents a real potential of the structure.

study we concentrate on the optical transitions related to the heavy-hole states, and therefore we have chosen the structures which are grown on $Cd_{0.96}Zn_{0.04}Te$ substrates to separate the heavy- and the light-hole states.

The energy separations between the confined levels in a QW structure decrease with increasing well width. When the energy separations between the confined levels are much smaller than the exciton binding energy, the exciton cannot be described by using a single electron band and a single hole band. The mixing between the different pairs of electron and hole bands has to be taken into account. Another convenient way to describe the exciton states is to introduce the concept of the quantization of the excitonic centre-of-mass motion (CM quantization) [17, 18], where the exciton corresponding to the fundamental band gap is first formed, then the centre-of-mass motion of such an exciton is further quantized by the well potential. The different exciton states can be roughly described by the following expression derived from an approximation with an infinite barrier potential [17]:

$$E_n = E_T + \frac{1}{2M^*}\left(\frac{\pi\hbar}{L}n\right)^2 \tag{1}$$

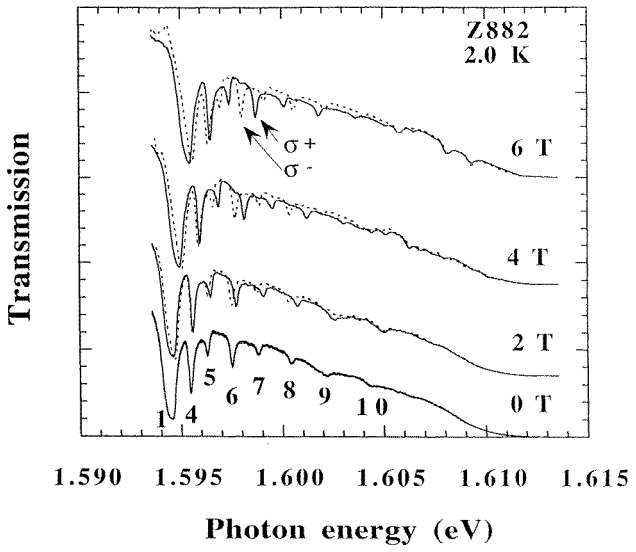

Figure 3. Transmission spectra of sample Z882 in four different magnetic fields, measured at 2.0 K. The polarization is defined with respect to the magnetic field.

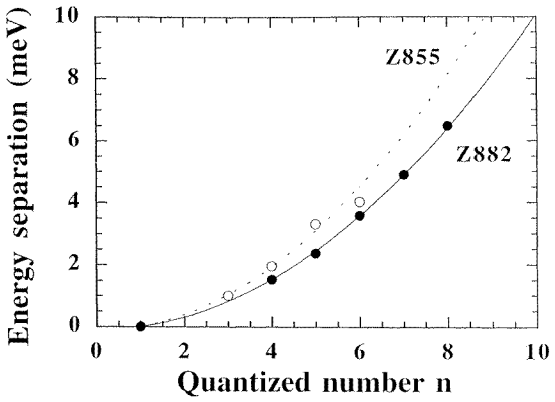

Figure 4. The energy separation between the ground and the excited CM excitons versus the quantization number n. The solid (Z882) and dotted (Z885) lines are calculated according to equation (1) in the text with $L_z = 240$ ML and 213 ML, respectively.

where M^* is the effective centre of mass of the exciton and is given by

$$M^* = m_e^* + \frac{m_0}{(\gamma_1 - 2\gamma_2)}$$

and n is the quantization number. E_T is the energy of the fundamental exciton transition. In a practical case, the effects due to the finite barrier potential have to be considered. Since the heavy-hole valence band offset (136 meV) and conduction band offset (300 meV) in the $CdTe/Cd_{0.75}Mg_{0.25}Te$ system are significantly larger than the confined energy, equation (1) is a very good approximation. On the other hand, for the CdTe/CdZnTe system one has to consider the finite-barrier effects. A systematic study of the CM quantization effects

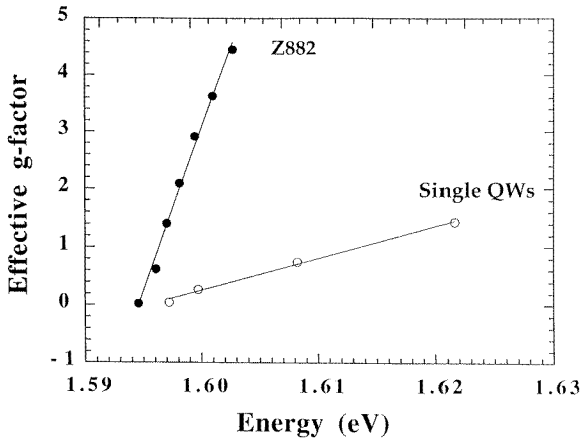

Figure 5. Effective g-factors of the exciton transitions deduced from transmission measurements for sample Z882. The g-factors of the fundamental excitons from four single $CdTe/Cd_{0.75}Mg_{0.25}Te$ QW structures (with well widths of 89 ML, 65 ML, 40 ML and 25 ML) are also included for comparison.

in the CdTe/CdZnTe system has been reported previously [17], and it is concluded that the CM quantized excitons appear when the well width is larger than about 200 Å in the CdTe/CdZnTe heterostructure. The more sophisticated theoretical treatment concerning the CM quantized exciton is a complicated problem [18], and particularly in our case where the structures contain fractional ML insertions. We will use equation (1) to discuss our results just for reasons of simplicity. From equation (1) it can be seen that the energy separations of the CM quantized excitons relative to ground exciton state ($n = 1$) have quadratic dependence on the quantization number n. This characteristic relation can be used to distinguish the CM quantized excitons and other excitons. Of course we have to be very careful in our case when the structures contain fractional ML ZnTe insertions, and in the case of $CdTe/Cd_{0.92}Zn_{0.08}Te$ QW the band offset is not so much greater than the CM quantized energy. We would expect to see some deviation from such a quadratic energy relation for the higher CM quantized exciton states. Figure 3 shows the transmission spectra from the reference sample Z882 at different magnetic fields. A series of sharp exciton transitions appears above the energy 1.59 eV. It can be seen from the figure 4 that these transitions follow the relation given by equation (1), as we expected that equation (1) would be a good approximation for the CdTe/CdMgTe system. It is clearly demonstrated that these exciton states in sample Z882 belong to the CM quantized excitonic transitions. In the presence of a magnetic field along the growth direction, each transition splits into two components that are circularly polarized (σ^- and σ^+). The splitting energy ΔE is characterized by an effective g-value (g_{eff}) by the relation

$$\Delta E = g_{eff} B \mu_B \tag{2}$$

where μ_B and B are the Bohr magneton and magnetic field, respectively. The effective g-value increases with increasing energy relative to the ground exciton state ($n = 1$) as can be seen from figure 5, and shows a linear dependence on the energy of the centre-of-mass quantization states. Such an energy dependence of the effective g-value can be used as another characteristic relation to distinguish between the CM quantized exciton states and the other exciton states. The effective g-value of the latter will be smaller, as can be seen

also in figure 5, where the effective g-values of the excitons in single CdTe/CdMgTe QW are included to compare with the g-values of the CM quantized excitons. The electron g-factors of the exciton transition (up to $n = 6$ which appears in PL spectra) have been measured by spin-quantum-beat experiments, which have been shown to be a powerful technique for measuring the electron g-factor [19–21]. The results show that the electron g-factors are the same. This means that the change of the CM exciton effective g-factors with increasing quantization numbers is due to the change of the hole g-factor involved. We will return to this point when we discuss the structures containing ZnTe insertions in the next section.

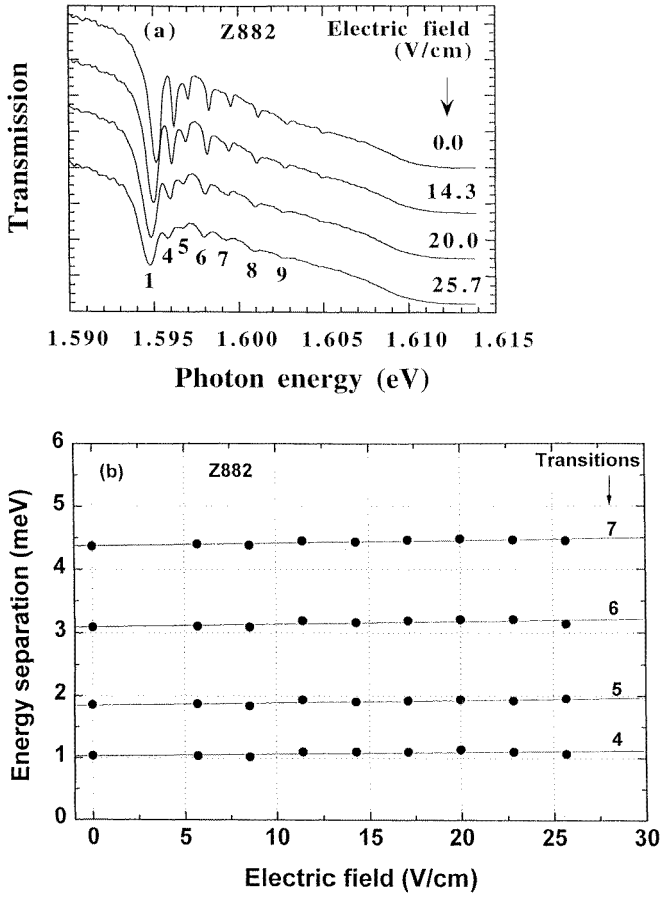

Figure 6. (a) Transmission spectra of sample Z882 in different applied electric fields. (b) The energy separation between the ground and the excited CM excitons versus applied electric fields.

The structure Z882 subjected to a weak electric field is also investigated. Figure 6(a) shows the transmission spectra of sample Z882 at different electric field strengths. The value of the electric field strength across the structure is calibrated according to the fundamental band-gap shift. The results show that the CM quantized excitons become weaker with increasing electric field strengths. Furthermore, the energy separations between the excited CM exciton states and the ground state increase with an increase in the electric field, as shown in figure 6(b). The above results are consistent with the localization effects introduced

by an applied electric field, i.e. applied electric fields reduce the freedom of exciton motion along the electric field direction. This means a slight reduction in the effective well width and weakening of the oscillator strength of the exciton recombination. This result shows that the CM exciton is very sensitive to potential perturbation along the direction of the excitonic centre-of-mass motion, as expected. Note that the applied electric field is extremely weak, and the maximum electric field strength used only causes a 0.2 meV shift of the fundamental exciton transition ($n = 1$).

4. The effects of a fractional monolayer of ZnTe inserted in the structures

Since any perturbation of the coherent motion of the exciton along the z-direction will strongly influence the CM quantized states, we now consider structures with a fractional ML of ZnTe inserted in a wide single QW.

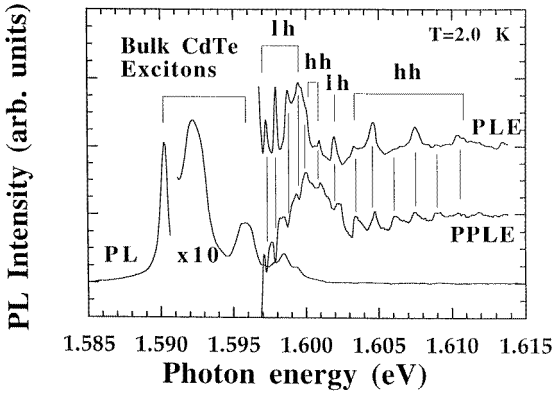

Figure 7. PL, PLE and PPLE spectra of sample Z852, measured at 2.0 K. Sample Z852 was grown on a CdTe substrate; the confined excitons appear at an energy above the CdTe free-exciton energy. The lh and hh characters of these confined excitons are indicated in the figure.

To illustrate the complicated exciton transitions observed in the structures grown on CdTe substrates due to both heavy- and light-hole states being involved in same spectral region, figure 7 shows the PL, PLE and PPLE spectra from sample Z852. A large number of exciton transitions appear above the CdTe free-exciton transition in PLE and PPLE spectra with a strong broad-background modulation from the bulk CdTe excited exciton state in the energy region between 1.598 eV and 1.604 eV. By using the knowledge obtained from our previous study on single-ZnTe-insertion CdTe QW structures [16] and polarized PLE data, we are able to identify the hh and lh characters of each transition appearing in the spectra. The lh excitons appear in a lower energy region than the hh excitons. This is due to localization effects introduced by the ZnTe insertion potential [16]. A series of the hh and lh excitons in the spectra is related to the CM excitons. It seems that the observed transitions are from more than one domain since the series of the hh and lh excitons is difficult to correlate with one set of the CM quantized excitons. To avoid the complication due to the hh and lh overlapping and its interference with CdTe substrate transitions, we will mainly concentrate on structures grown on a CdZnTe substrate. As we mentioned earlier, due to the strain splitting, the fundamental band edge for the lh state is more than 10 meV higher than that of the hh state for the substrate with 4% Zn, and the energy region of the hh exciton transitions also becomes transparent.

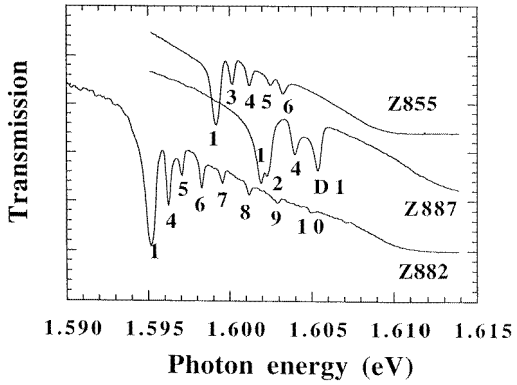

Figure 8. Transmission spectra of samples Z887 and Z885, measured at 2.0 K. The spectrum from reference sample Z882 is also included for comparison.

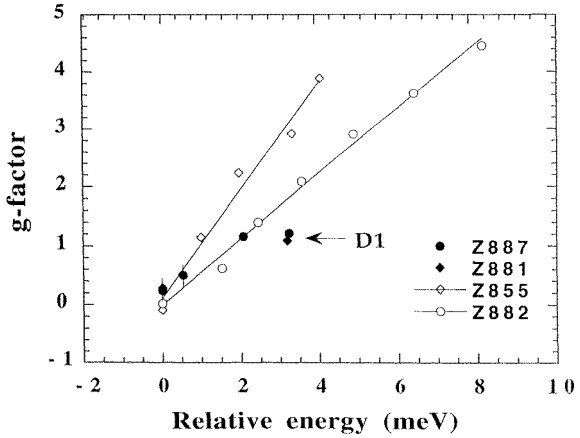

Figure 9. Effective g-factors of the exciton transitions from samples Z887, Z885 and Z881 in comparison with the g-factors of the CM quantized excitons from reference sample Z882.

The transmission spectra from samples Z855 and Z887 are shown in figure 8 together with the spectra from reference sample Z882. First there is a blue shift of the fundamental excitonic transition from samples Z887 and Z855 in comparison with the transition from reference sample Z882. Secondly, the numbers of the observed exciton transitions are reduced for the structures with the ZnTe insertions in comparison with reference sample Z882. To identify the transitions observed in samples Z855 and Z887, transmission spectra in the presence of a magnetic field have been measured. The effective g_{eff}-value of each transition deduced according to equation (2) is presented in figure 9 in comparison with the g-value of the CM quantized excitons from sample Z882. The g-values of the transitions in sample Z855 show a good linear energy relation; this indicates that the observed transitions originate from the CM quantization. This is also consistent with the CM characteristic energy relation as shown in figure 4. For sample Z887, the results show that the g-value of transition D1 does not follow the linear energy relation (see figure 9). This indicates that transition D1 does not originate from the CM quantization and is more probably related to

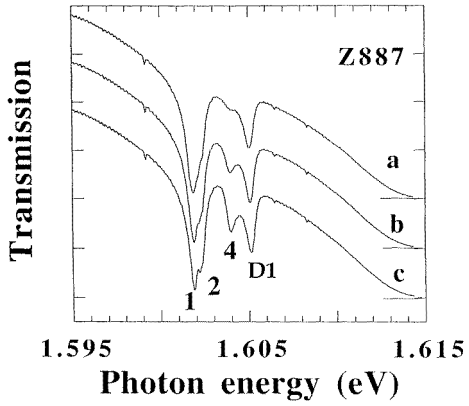

Figure 10. Transmission spectra of sample Z887 under different illumination conditions: (a) dark; (b) 0.1 mW; and (c) 0.5 mW. The light is defocused to about 2×2 mm^2 to illuminate the sample.

an exciton formed from a higher pair of confined subbands or a localized exciton resulting from a disorder effect related to the ZnTe insertions. To further characterize the transitions 2, 4 and D1, figure 10 shows the transmission spectra from sample Z887 under different illumination conditions. The illumination source is a multiple-line output of an Ar^+ laser. With increasing excitation power, the transitions labelled 2 and 4 become stronger, while the other transmission peaks are not influenced. This fact further indicates that the origin of the transition D1 is different from that of transitions 2 and 4. Since such weak illumination can only slightly modify the band bending across the structures towards a flatter-band condition, this means that transitions 2 and 4 are very sensitive to small changes of the band potential along the growth direction. This fact is consistent with an identification of transitions 2 and 4 as originating from the CM quantization, and is consistent with the results presented in section 3 for the weak electric field dependence of the CM quantized excitons.

Table 2. The fundamental hh exciton transition energies from experimental measurements (Exp. $\pm$ 0.0002 eV) and the calculations (Calc.), the electron g-factors ($g_e \pm 0.005$) and the calculated hh exciton binding energy (ΔE_{ex}) for the different structures.

	Z882	Z887	Z881	Z879	Z855	Z927	Z852
Exp. (eV)	1.5948	1.6018	1.6009	1.6022	1.5992	1.6012	1.5995
Calc. (eV)	1.5948	1.6025	1.6009	1.6030	1.5999	1.6013	1.6001
ΔE_{ex} (meV)	10.88	11.14	11.01	11.16	10.83	10.92	11.12
g_e	−1.601	−1.552	−1.553	−1.551	−1.557	−1.555	

To gain more information about the contribution of the electron and the hole g-factors in the effective g_{eff}-factors of the CM quantized excitons, we have performed spin-quantum-beat measurements. In this method, the Larmor angular frequency ω_L is directly correlated with the absolute value of g_e^* as $\omega_L = |g_e^*|\mu_B B/\hbar$, and ω_L can be measured through the time-varying circular polarization of the photoluminescence emitted along the growth direction after excitation by a short, circularly polarized laser pulse (for details see references [19, 20]). Figure 11 shows typical spin-quantum beats measured at 12 K and 1.5 T for sample Z855 after excitation by a short laser pulse (∼10 ps) at 710 nm. The excitation intensity

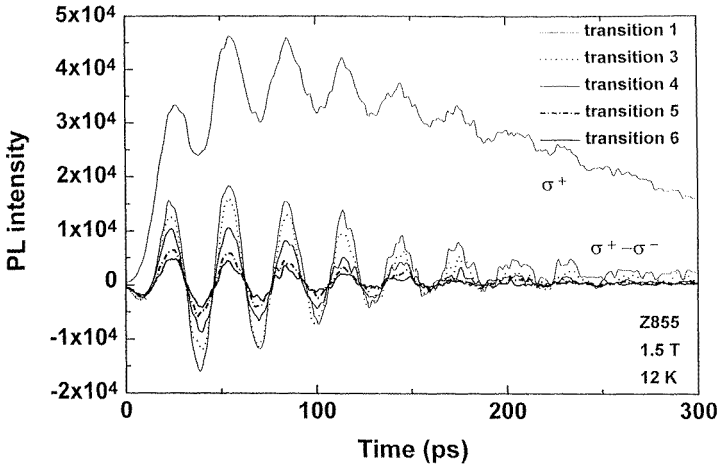

Figure 11. Typical spin-quantum beats for sample Z885 at 1.5 T and 12 K. The difference between σ^+ and σ^- is measured with detection at different exciton transitions.

is 9 mW. The PL signal shows oscillations as a consequence of the Larmor precession of the electron spins in the magnetic field. The period τ of such oscillations is governed by ω_L in the relation $\tau = 2\pi/\omega_L$. Therefore, the absolute value g_e^* can be deduced by measuring the period τ of the time-varying circular polarization of the photoluminescence as shown in figure 11. Since the oscillations of the σ^+- and σ^--components are shifted by π in phase [19], the differences between the σ^+- and σ^--transitions are measured to enhance the experimental accuracy as shown in figure 11. The different curves in figure 11 correspond to the detection at the different exciton transitions labelled according to figure 8. It is clearly shown that within the experimental accuracy the oscillation period is the same, which means that the electron g-factor is the same for all CM excitons in Z855. To improve the experimental accuracy, we have measured the period τ of such oscillations in different magnetic fields in the region from 1 T to 2.5 T; then the electron g-factor is deduced from the field dependence. Again the same electron g-factor is obtained for the different CM excitons. The measured electron g-factors from different samples are summarized in table 2. The smaller variation of the electron g-factor from sample to sample may be due to the difference of the effective Zn concentrations, wave-function leakage into the barrier material and different strain effects in the structures.

4.1. Effects of growth temperatures

Since the growth temperature is one of the most important factors that influences the island formation in the xy-plane [22], we can change the growth temperature to see how the exciton transitions are influenced. Two groups of samples have been used for this purpose. The first pair of samples are Z855 and Z927, which have similar structures but have been grown at the temperatures 320 °C and 210 °C, respectively. The transmission spectra from these two samples are shown in figure 12. The sharp CM quantized excitons observed in sample Z855 disappear in sample Z927. Note that sample Z927 was grown on a $Cd_{0.95}Zn_{0.05}Te$ substrate, and thus light can be transmitted at energy above 1.608 eV through sample Z927. The second group of samples is Z887, Z879 and Z881, which also have similar structures but are grown at the temperatures 320 °C, 280 °C and 240 °C, respectively. Figure 13 shows

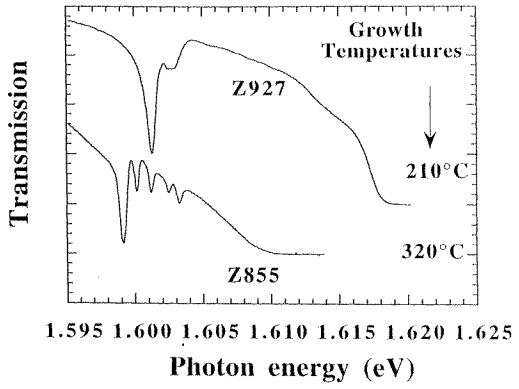

Figure 12. Transmission spectra of samples Z855 and Z927, measured at 2.0 K. Two samples are designed to have similar structures but were grown at different temperatures. Notice that sample Z927 was grown on a $Cd_{0.95}Zn_{0.05}Te$ substrate, instead of $Cd_{0.96}Zn_{0.04}Te$.

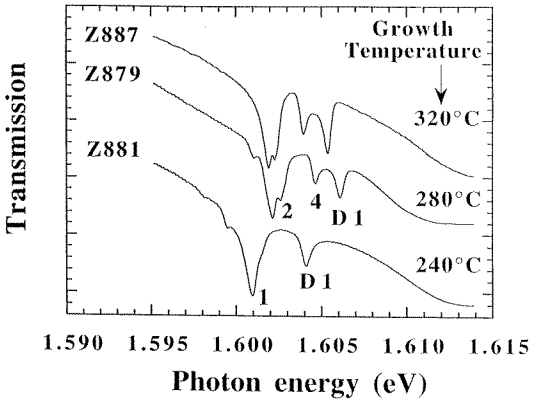

Figure 13. Transmission spectra of samples Z887, Z879 and Z881, measured at 2.0 K. Three samples are designed to have similar structures but were grown at different temperatures.

transmission spectra for these three samples. The results also clearly illustrate that the CM quantized exciton states disappear in sample Z881 which was grown at a low temperature.

Transmission spectra from the above two groups of samples clearly demonstrate that the exciton transitions are strongly influenced by the growth temperature. The CM excitons are only observable in the structures grown at temperatures above 280 °C. The presence of such mobile CM quantized excitons in the structures grown at the higher temperatures (>280 °C), which are very sensitive to disorder, indicates that the energy fluctuations associated with the ZnTe islands are organized in a coherent way. When the growth temperature is reduced to below 240 °C, the CM quantized effects disappear and only the localized excitons are observed. This shows that kinetic barriers limit the surface diffusion and prevent the formation of an ordered state. Since at low growth temperatures (such as 240 °C for sample Z881 and 210 °C for sample Z927) the ZnTe island size becomes smaller and irregular with a random distribution in the xy-plane; the motion of the exciton in the xy-plane feels a perturbation, resulting in exciton localization in the plane. Due to the random distribution

of the position and size of the ZnTe islands in the xy-plane for each insertion, the exciton cannot move coherently across the five insertions along the growth direction. The CM quantization is then difficult to observe. On the other hand, at a high growth temperature (320 °C for samples Z887 and Z855, and 280 °C for Z879) the equilibrium growth condition is reached. Then ZnTe islands with a coherent distribution and a regular size are formed. The excitons can move coherently across the five insertions along the growth direction, resulting in the observation of the CM quantized excitons (samples Z887, Z879 and Z855).

The time-resolved measurements further support this explanation. The decay times of transition 1 for samples Z887 and Z881 are 260 ps and 340 ps, respectively. The longer decay time of the free exciton in sample Z881 grown at 240 °C means that additional localization is involved in the free-exciton recombination. This fact is consistent with the formation of a disordered state at low growth temperatures and an ordered state at high growth temperatures.

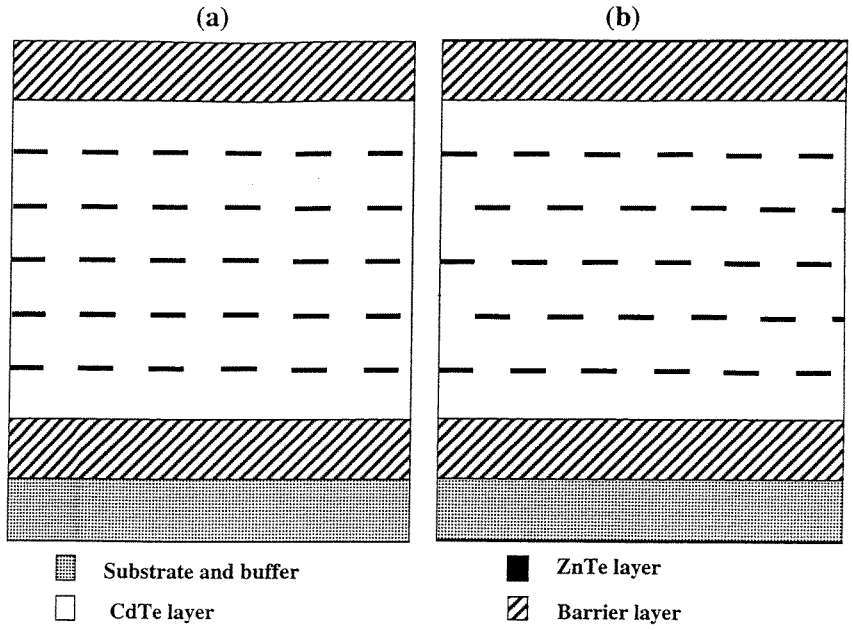

Figure 14. A schematic view of the possible self-organizing distributions of the ZnTe islands in a CdTe matrix: (a) vertical stacking of the ZnTe islands; (b) a staggered line-up of the ZnTe islands.

4.2. The model of the coherent arrangement of ZnTe islands

There are two possibilities shown in figure 14 for the coherent distribution of the inserted ZnTe along the growth direction. One is the correlated vertical stacking of the ZnTe islands that is obtained if the interaction is attractive (figure 14(a)). The other one is the staggered (or anticorrelated) line-up that is obtained if the interaction between islands is repulsive (figure 14(b)). From our experimental results we cannot exclude either of them since we have no information about the island size. From the recent study of narrow CdTe QW (15 nm) with half monolayers of ZnTe inserted in symmetric or asymmetric positions in the well, the observation of parity-forbidden transitions when two half-monolayers of ZnTe

are placed in symmetric positions provides an indication that the inserted ZnTe islands may favour a staggered line-up [23]. The correlated vertical stacking alignment has been directly observed in the case of InAs islands inserted in a GaAs matrix by the transmission electron microscope (TEM), and such vertical alignment has been explained as due to strain effects created by embedded InAs islands which exhibit a lattice mismatch to the GaAs matrix [5].

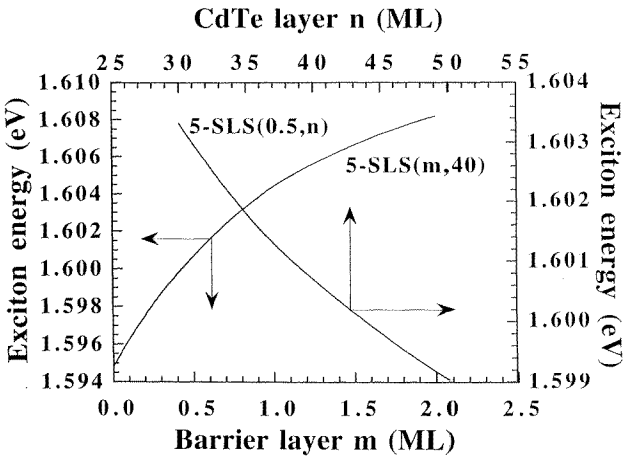

Figure 15. The theoretical calculated hh exciton transition energy versus the barrier layer thickness for 5-SLS(m, 40) structures and versus the CdTe layer thickness for 5-SLS(0.5, n) structures.

5. Theoretical simulations and discussions

To compare the theoretical calculations with experimental energy values of the fundamental exciton transition, we have performed the following simple effective-mass calculations. Exacerbating the effect of the uncertainty of the parameters used in the calculation, the exciton trial function is poor for wide wells, so the following calculated results can only be used as a guide. The confined electron and hole levels in the structures are obtained by numerically solving the effective-mass Schrödinger equation

$$H_k\varphi_n(Z_k) = E_n\varphi_n(Z_k)$$
$$H_k = \left(-\frac{\hbar^2}{2}\frac{\partial}{\partial Z_k}\frac{1}{m_k^*}\frac{\partial}{\partial Z_k} + V(Z_k)\right) \tag{3}$$

where $k \in$ (e, hh, lh). The hh and lh effective mass m^* are given by

$$\frac{m_0}{\gamma_1 - 2\gamma_2} \qquad \text{and} \qquad \frac{m_0}{\gamma_1 + 2\gamma_2}$$

respectively. $V(Z_k)$ is the potential of the structures with properly included strain effects [16]. The parameters used in our calculations can be found in our previous paper where coupled double-QW structures were investigated [16]. The exciton effects have been considered in our calculations by simply using the two-band model for the hh exciton. The exciton wave functions are taken as

$$\psi_{ex}^n = \varphi_n(Z_e)\varphi_n(Z_h)\exp(-\lambda\sqrt{\rho^2 + (Z_e - Z_h)^2}) \tag{4}$$

and the exciton Hamiltonian can be written as $H_{ex} = H_e + H_{hh,lh} + H_{eh}$, where H_e and $H_{hh,lh}$ are the free-electron and the free-hole Hamiltonians in the structures, respectively, as defined in equation (3). $\varphi_n(Z_e)$ and $\varphi_n(Z_h)$ are the electron and the hole wave functions corresponding to the nth subband in the QW structures. In cylindrical coordinates the electron–hole interaction Hamiltonian is given by

$$H_{eh} = -\frac{\overline{h}^2}{2\mu_{hh,lh}}\frac{1}{\rho}\frac{\partial}{\partial\rho}\left[\rho\frac{\partial}{\partial\rho}\right] - \frac{e^2}{4\pi\varepsilon_0\varepsilon_r\sqrt{\rho^2 + (Z_e - Z_{hh,lh})^2}}$$

where $m_{hh,lh}$ are effective masses of the heavy- and the light-hole excitons in the plane perpendicular to the growth direction, given by

$$\frac{1}{\mu_{hh,lh}} = \frac{1}{m_e^*} + \frac{\gamma_1 \pm \gamma_2}{m_0}$$

where $+$ and $-$ correspond to the hh and the lh states respectively. The exciton transition energy is given by varying the parameter λ to minimize the exciton energy

$$E_{ex}^n = \frac{\langle\psi_{ex}^n|H_{ex}|\psi_{ex}^n\rangle}{\langle\psi_{ex}^n|\psi_{ex}^n\rangle}.$$

As demonstrated in figure 2(b), fractional ML ZnTe insertions in a wide CdTe/CdMgTe single QW can strongly modify the wave functions both for electrons and for holes. To illustrate the effects of the ZnTe insertions, figure 15 shows the hh exciton transition energy versus the thickness (m) of the inserted ZnTe layers for the structures 5-SLS(m, 40), as well as the hh exciton transition energy versus thickness (n) of the CdTe layer for the structures 5-SLS(0.5, n). It is clearly shown that the hh exciton energy is very sensitive to the thickness variation of the ZnTe layer. With 0.5 ML thickness of the inserted ZnTe layers, the fundamental exciton transition has already shifted toward higher energy by about 6 meV. On the other hand, the hh exciton energy is less sensitive to the variation of the CdTe layer. For comparison with experimental results, the fundamental exciton transition for each of the structures is calculated, and these are listed in table 2 together with the experimental values.

6. Summary

In summary, we have presented optical investigations of fractional monolayers of ZnTe inserted in a wide CdTe/$Cd_{0.75}Mg_{0.25}$Te QW structure. The inserted ZnTe layers have a strong influence on the exciton transitions. We demonstrate, by monitoring the CM quantized exciton transition, that an ordered distribution of the inserted ZnTe islands is formed at a growth temperature higher than 280 °C, while the distribution of the ZnTe islands is random for a growth temperature lower than 240 °C. We found experimentally that the effective g-factor of the CM excitons increases strikingly on increasing the quantization number, while the electron g-factor involved is unchanged. This leads to the conclusion that the change of the effective g-factor of the CM excitons is due to the change of the hole g-factor involved.

There are a number of issues that remain for further investigation. In particular, the theoretical calculations of the g-factors of the CM quantized excitons and the theoretical calculations of the free-hole g-factors in such strained superlattice structures remain to be properly performed. Secondly, a proper theoretical calculation of the CM exciton transitions is necessary for such fractional-ML-inserted QW structures. Finally, experimental work using transmission electron microscopes could directly provide us with the accurate configuration of the island distribution and the sizes of the islands.

Acknowledgments

We would like to thank R T Cox for valuable discussion and comments. One of the authors (QXZ) would like to thank J Weber for hospitality at the Max-Planck-Institut in Stuttgart, where the time-resolved measurements were carried out. M Oestreich at the Max-Planck-Institute in Stuttgart is also acknowledged for assisting in the time-resolved measurements.

References

[1] Yao J Y, Andersson T G and Dunlop G L 1991 *J. Appl. Phys.* **69** 2224
[2] Leonars D, Krishnamurthy M, Reaves C M, Denbaars S P and Petroff P M 1993 *Appl. Phys. Lett.* **63** 3203
[3] Nötzel R, Fukui T and Hasegawa H 1994 *Appl. Phys. Lett.* **65** 2854
[4] Moison J M, Houzay F, Barthe F and Leprince L 1994 *Appl. Phys. Lett.* **64** 196
[5] Xie Q, Madhukar A, Chen P and Kobayashi N P 1995 *Phys. Rev. Lett.* **75** 2542
[6] Ledentsov N N 1996 *Proc. 23rd Int. Conf. on the Physics of Semiconductors (Berlin)* vol 1 (Singapore: World Scientific) p 19
[7] Huan T S and Iyer S S 1991 *Appl. Phys. Lett.* **59** 2242
[8] Mo Y W, Swartzentruber B S, Kariotis R, Webb M B and Lagally M G 1989 *Phys. Rev. Lett.* **63** 2393
[9] Tersoff J, Teichert C and Lagally M G 1995 *Phys. Rev. Lett.* **76** 1675
[10] Zeppenfeld P, Krzyzowski M, Romainczyk C, Comsa G and Lagally M G 1994 *Phys. Rev. Lett.* **72** 2737
[11] Magnea N 1994 *J. Cryst. Growth* **138** 550
[12] Zhao Q X, Magnea N and Pautrat J L 1996 *J. Cryst. Growth* **159** 425
[13] Trzeciakowski W, Hawrylak P, Aers G C and Nurmikko A V 1989 *Solid State Commun.* **71** 653
[14] Kuhn-Heinrich B, Ossau W, Heinke H, Fisher F, Litz T, Waag A and Landwehr G 1993 *Appl. Phys. Lett.* **63** 21
[15] Peyla P, Merle d'Aubigné Y, Wasiela A, Romestain R, Mariette H, Sturge M D, Magnea N and Tuffigo H 1992 *Phys. Rev.* B **46** 1557
[16] Zhao Q X, Magnea N and Pautrat J L 1995 *Phys. Rev*. B **52** 16 612
[17] Tuffigo H 1991 *Optics of Excitons in Confined Systems (Inst. Phys. Conf. Ser. 123)* (Bristol: Institute of Physics Publishing) p 37
[18] Tomassini N, D'Andrea A, Del Sole R, Tuffigo-Ulmer H, and Cox R T 1995 *Phys. Rev.* B **51** 5005
[19] Heberle A P, Rühle W W and Ploog K 1994 *Phys. Rev. Lett.* **72** 3887
[20] Oestreich M and Rühle W W 1995 *Phys. Rev. Lett.* **74** 2315
[21] Zhao Q X, Oestreich M and Magnea N 1996 *Appl. Phys. Lett.* **69** 3704
[22] Lagally M G 1993 *Phys. Today* **46** (11) 24
[23] Calvo V, Lefebvre P, Allègre J, Bellabchara A, Mathieu H, Zhao Q X and Magnea N 1996 *Phys. Rev*. B **53** R16 164